

# Complexes of Bis-*ortho*-cyclometalated Bisphosphinoaryl Ruthenium(II) Cations with Neutral *Meta*-bisphosphinoarene Ligands Containing an Agostic C–H···Ru Interaction<sup>†</sup>

Paulo Dani, Mieke A. M. Toorneman, Gerard P. M. van Klink, and Gerard van Koten\*

Department of Metal-Mediated Synthesis, Debye Institute, Utrecht University, Padualaan 8, 3584 CH Utrecht, The Netherlands

Received June 7, 2000

The synthesis, characterization, and reactivity of various ruthenium(II) complexes [Ru(R–PCP)(R'–PCHP)][OTf] are presented. These complexes are highly dissymmetric and show fluxional behavior in solution. They contain one monoanionic,  $\eta^3$ -*P,C,P*-tridentate-bonded bisphosphinoaryl ligand (R–PCP = [C<sub>6</sub>H<sub>2</sub>(CH<sub>2</sub>PPh<sub>2</sub>)<sub>2</sub>-2,6-R-4]<sup>–</sup>; R = H or Br) and one neutral, *trans*-*P,P*-bidentate-bonded bisphosphinoarene ligand (R'–PCHP = C<sub>6</sub>H<sub>3</sub>(CH<sub>2</sub>PPh<sub>2</sub>)<sub>2</sub>-3,5-R'-1). The C–H bond that is *ortho* to both CH<sub>2</sub>PPh<sub>2</sub> substituents of the bidentate-bonded ligand is interacting with the metal center (i.e., has an agostic contact with the cationic ruthenium center). The location of the agostic proton in the <sup>1</sup>H NMR spectrum as well as the three-dimensional structure of these complexes in solution was obtained by means of several two-dimensional NMR techniques (<sup>1</sup>H–<sup>1</sup>H COSY, <sup>31</sup>P–<sup>1</sup>H COSY, <sup>13</sup>C–<sup>1</sup>H COSY, <sup>1</sup>H NOESY, <sup>1</sup>H ROESY, and <sup>31</sup>P EXSY). The <sup>1</sup>J<sub>HC</sub> of the agostic contact amounted to 112 Hz, which represents a reduction of 46 Hz in relation with the same coupling for this C–H bond in the free ligand. Furthermore, the molecular geometry of [Ru(H–PCP)(PCHP)][OTf] in the solid state was established by single-crystal X-ray diffraction techniques, and the structural features corroborate with the observations in solution. In the complex [Ru(H–PCP)(Br–PCHP)][OTf], interconversion of the cyclometalated and neutral bisphosphine ligands via exchange of the agostic hydrogen atom from the neutral to the cyclometalated carbon to yield [Ru(Br–PCP)(H–PCHP)][OTf] was observed. A mechanistic proposal based on an aromatic electrophilic substitution is discussed. Moreover, the reaction of [Ru(OSO<sub>2</sub>CF<sub>3</sub>)(NCN)(PPh<sub>3</sub>)] (NCN = [C<sub>6</sub>H<sub>3</sub>(CH<sub>2</sub>NMe<sub>2</sub>)<sub>2</sub>-2,6]<sup>–</sup>) with the neutral bisphosphinoarene resulted in the quantitative formation of the new cyclometalated species [Ru(R–PCP)(R–PCHP)][OTf] with the net loss of the neutral bisaminoarene ligand NCHN and PPh<sub>3</sub>.

## Introduction

The cyclometalation of bidentate ligands is thought to involve  $\eta^2$ -*E,E* species (E = N, P, As, S) as crucial intermediates,<sup>1–18</sup> and there are situations where it has

been claimed to have unequivocally established the involvement of such species in the process of C–M bond formation.<sup>1,5,8,13,19</sup> The participation of such intermediates is considered feasible for the following reasons: (i) chelation of a polydentate ligand is known to be thermodynamically favored over open-chain structures; (ii) chelation brings the carbon atom to be metalated in close proximity of the metal center; (iii) the metalated carbon atom is generally situated in that part of the

\* To whom correspondence should be addressed. E-mail: g.vankoten@chem.uu.nl. Fax: +(31) 30 2523615.

<sup>†</sup> Dedicated to Professor Dr. H. Günther (Universität-Gesamthochschule Siegen, Siegen, Germany) on the occasion of his 65th birthday.

(1) Bennett, M. A.; Johnson, R. N.; Tomkins, I. B. *J. Organomet. Chem.* **1977**, *128*, 73–84.

(2) Crocker, C.; Errington, R. J.; Markham, R.; Moulton, C. J.; Shaw, B. L. *J. Chem. Soc., Dalton Trans.* **1982**, 387–395.

(3) Cross, R. J.; Kennedy, A. R.; Manojlovic-Muir, L.; Muir, K. W. *J. Organomet. Chem.* **1995**, *493*, 243–249.

(4) Rimml, H.; Venanzi, L. M. *J. Organomet. Chem.* **1983**, *259*, C6–C7.

(5) Karlen, T.; Dani, P.; Grove, D. M.; Steenwinkel, P.; van Koten, G. *Organometallics* **1996**, *15*, 5687–5694.

(6) Ogasawara, M.; Saburi, M. *Organometallics* **1994**, *13*, 1911–1917.

(7) Steenwinkel, P.; Kolmschot, S.; Gossage, R. A.; Dani, P.; Veldman, N.; Spek, A. L.; van Koten, G. *Eur. J. Inorg. Chem.* **1998**, 477–483.

(8) Lesueur, W.; Solari, E.; Floriani, C.; Chiesi-Villa, A.; Rizzoli, C. *Inorg. Chem.* **1997**, *36*, 3354–3362.

(9) Gozin, M.; Welsman, A.; Ben-David, Y.; Milstein, D. *Nature* **1993**, *364*, 699–701.

(10) Gozin, M.; Aizenberg, M.; Liou, S.-Y.; Welsman, A.; Ben-David, Y.; Milstein, D. *Nature* **1994**, *370*, 42–44.

(11) Liou, S.-Y.; Gozin, M.; Milstein, D. *J. Chem. Soc., Chem. Commun.* **1995**, 1965–1966.

(12) van der Boom, M. E.; Kraatz, H.-B.; Ben-David, Y.; Milstein, D. *Chem. Commun.* **1996**, 2167–2168.

(13) Rybtchinski, B.; Vigalok, A.; Ben-David, Y.; Milstein, D. *J. Am. Chem. Soc.* **1996**, *118*, 12406–12415.

(14) Gandelman, M.; Vigalok, A.; Shimon, L. J. W.; Milstein, D. *Organometallics* **1997**, *16*, 3981–3986.

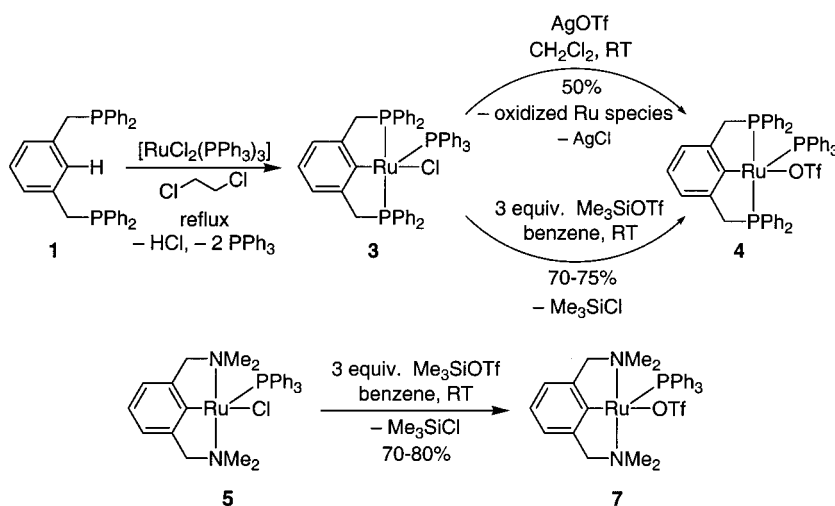
(15) Rybtchinski, B.; Ben-David, Y.; Milstein, D. *Organometallics* **1997**, *16*, 3786–3793.

(16) van der Boom, M. E.; Liou, S.-Y.; Ben-David, Y.; Gozin, M.; Milstein, D. *J. Am. Chem. Soc.* **1998**, *120*, 13415–13421.

(17) van der Boom, M. E.; Liou, S.-Y.; Ben-David, Y.; Shimon, L. J. W.; Milstein, D. *J. Am. Chem. Soc.* **1998**, *120*, 6531–6541.

(18) Rybtchinski, B.; Milstein, D. *Angew. Chem., Int. Ed.* **1999**, *38*, 870–883.

## Scheme 1. Synthesis of Ruthenium Triflate Complexes



ligand skeleton that is located between both donor heteroatoms; and finally (iv) cyclometalation of the ligand is generally a highly stereoselective process.

Here, we report the results of our investigations involving the aryl ligands  $C_6H_3(CH_2PPh_2)_{2-3,5-R-1}$ , abbreviated as R-PCHP (**1**, R = H; **2**, R = Br), and the ruthenium-triflate complexes  $[Ru(OTf)(C_6H_3\{CH_2E\}_{2-2,6})(PPh_3)]$  (**4**, E =  $PPh_2$ ; **7**, E =  $NMe_2$ ;  $OTf = CF_3SO_3^-$ ). In addition, a unique example of a cationic complex,  $[Ru(H-PCP)(PCHP)][OTf]$ , was isolated containing both an  $\eta^3$ -P,C,P' tridentate-bonded PCP monoanion and a *trans*- $\eta^2$ -P,P' bidentate-bonded PCHP ligand. The  $\eta^2$ -P,P' ligand has one aromatic C-H bond coordinated to the metal center (i.e., has an agostic C-H-to-Ru contact).<sup>20</sup> Cross-experiments involving two different bis-phosphine ligands coordinated to the ruthenium cationic center suggest that agostic and metalated sites can exchange positions. A mechanism based on an aromatic electrophilic pathway is proposed for this process.

## Results and Discussion

**Synthesis of Ruthenium Triflate Complexes.** The formation of  $[RuCl(R-PCP)(PPh_3)]$  (R-PCP =  $[C_6H_2(CH_2PPh_2)_{2-2,6-R-4}]^-$ , R = H,<sup>5,21</sup> Ph,<sup>5</sup> Br;<sup>22</sup> see Scheme 1 for R = H (**3**)) complexes obtained from the reaction of  $[RuCl_2(PPh_3)_3]$  with the parent arene R-PCHP proceeds with net loss of HCl. The best results were obtained with 1,2-dichloroethane as solvent in terms of reaction time, yields, and the ease of workup of the resulting products.<sup>22</sup> In the case of  $[RuCl(PCP)(PPh_3)]$  (**3**, R-PCP with R = H, further abbreviated as PCP), replacement of the remaining chloride is achieved by reaction with AgOTf, thus forming **4** in 53% yield.<sup>5</sup> The reason for such moderate yield can be deduced from the resonances observed in the  $^{31}P$  NMR spectrum of the crude reaction mixture. In this spectrum in addition to a doublet and a triplet related to **4**, also a broad singlet

at ca. 29 ppm is found, which points to the presence of a byproduct. Interestingly, when the reaction solution was layered with benzene, a brown solid slowly precipitated, causing concomitant disappearance of the singlet detected in the  $^{31}P$  NMR spectrum. The  $^1H$  NMR spectrum of the brown solid in  $CD_2Cl_2$  consisted of broad resonances which remained unaffected by temperature variation in the range  $-100$  to  $+25$  °C, suggesting that the peak broadness was not caused by exchange (fluxional) processes but more likely by the presence of paramagnetic  $Ru^{III}$  species. The formation of this kind of oxidation product is often observed in halide abstraction reactions of electron-rich (i.e., late transition) metal complexes with silver salts. This occurs as a result of metal oxidation via an electron-transfer process, ultimately forming metallic (elemental) silver as a byproduct. An even more drastic situation was observed in the case of the analogous compounds  $[RuCl(NCN)(PPh_3)]$  (**5**,  $NCN = [C_6H_3(CH_2NMe_2)_{2-2,6}]^-$ ) and  $[Ru(NCN)(terpy)]Cl$  (**6**). Due to the  $\sigma$ -donating character of the dimethylamino groups, the ruthenium(II) center in these complexes is more prone to oxidation. Attempts to replace the chloride ligand in **5** by typical noncoordinating anions (e.g.,  $BF_4^-$  or  $OTf^-$ ) using the corresponding silver salt were not successful and resulted in complete decomposition of the starting materials. In case of **6** (and related complexes involving other types of NCN ligands), a selective oxidative reaction is observed leading to oxidation of both the metal center ( $Ru^{II}$  to  $Ru^{III}$ ) and the ligand framework.<sup>23-25</sup> The latter oxidation results in the formation of a new C-C bond, i.e., yielding ionic 4,4'-biphenylene-bridged bis-ruthenium complexes  $[Ru_2(4,4'-(C_6H_2\{CH_2NMe_2\}_{2-2,6})_2)(terpy)_2]^{n+}$  ( $n = 2, Ru^{II}, Ru^{II}$ ; and **4**,  $Ru^{III}, Ru^{III}$ ).

In contrast with the nonselective reactions with AgX, complexes **3** and **5** react selectively with a 3-fold excess of  $Me_3SiOTf$ <sup>26</sup> at room temperature (RT) to yield the corresponding triflate complexes **4** and **7**, respectively

(19) Baltensperger, U.; Gunter, J. R.; Kägi, S.; Kahr, G.; Marty, W. *Organometallics* **1983**, *2*, 571-578.

(20) (a) Brookhart, M.; Green, M. L. H.; Wong, L.-L. *Prog. Inorg. Chem.* **1988**, *36*, 1-124. (b) Crabtree, R. H.; Hamilton, D. G. *Adv. Organomet. Chem.* **1988**, *28*, 299-338.

(21) Jia, G.; Lee, H. M.; Williams, I. D. *J. Organomet. Chem.* **1997**, *534*, 173-180.

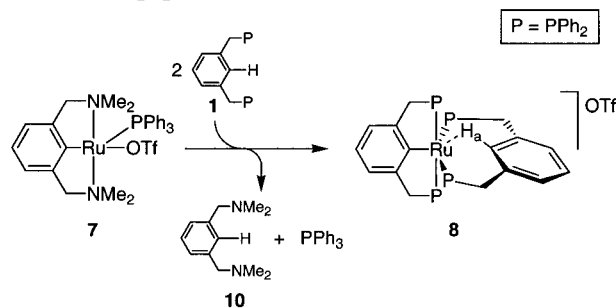
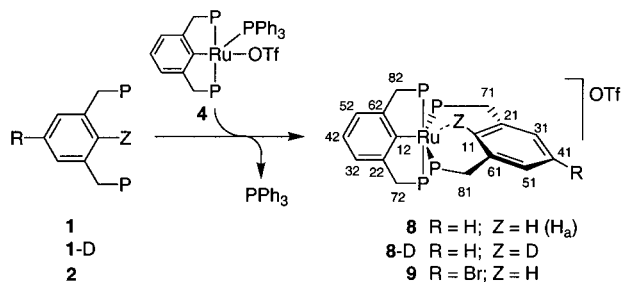
(22) Dani, P.; Richter, B.; van Klink, G. P. M.; van Koten, G. *Eur. J. Inorg. Chem.*, in press.

(23) Sutter, J.-P.; Grove, D. M.; Beley, M.; Collin, J. P.; Veldman, N.; Spek, A. L.; Sauvage, J. P.; van Koten, G. *Angew. Chem., Int. Ed. Engl.* **1994**, *33*, 1282-1285.

(24) Beley, M.; Collin, J.-P.; Louis, R.; Metz, B.; Sauvage, J.-P. *J. Am. Chem. Soc.* **1991**, *113*, 8521-8522.

(25) Beley, M.; Collin, J.-P.; Sauvage, J.-P. *Inorg. Chem.* **1993**, *32*, 4539-4543.

(26) Aizenberg, M.; Milstein, D. *J. Chem. Soc., Chem. Commun.* **1994**, 411.

**Scheme 2. Synthesis of Ru Complexes Containing an Agostic Contact**

(see Scheme 1). The only other products in the reaction are  $\text{Me}_3\text{SiCl}$  (a volatile liquid) and residual  $\text{Me}_3\text{SiOTf}$  (highly soluble in apolar solvents). Both of these latter materials can be easily removed.

The structure in solution of  $[\text{Ru}(\text{OTf})(\text{C}_6\text{H}_3\{\text{CH}_2\text{-NMe}_2\}_{2-2,6})(\text{PPh}_3)]$  (**7**) was established by its distinct  $^1\text{H}$  and  $^{31}\text{P}$  NMR spectra as well as by its reactivity toward the PCHP ligand (see below). Interestingly, complex **7** is stable for long periods (2 months) as a solution in benzene. However, in the solid state **7** slowly decomposes within one week to a brown benzene-insoluble solid.

**Reaction of Ruthenium–Triflate Complexes with R–PCHP Ligands.** Reaction of a solution of **4** in  $\text{CH}_2\text{Cl}_2$  with ligand **1** in a 1:1 molar ratio (see Scheme 2) at room temperature resulted in a rapid color change of the reaction solution from green to dark yellow. The  $^{31}\text{P}\{^1\text{H}\}$  NMR spectrum of this solution (RT) showed very broad signals between 15 and 45 ppm as well as a signal at ca.  $-4.5$  ppm. This latter signal points to the presence of free  $\text{PPh}_3$ . Workup of the reaction mixture led to the isolation of a yellow solid. The  $^{19}\text{F}\{^1\text{H}\}$  NMR spectrum (RT) showed one singlet resonance located at  $-73.41$  ppm, indicating the presence of a noncoordinated triflate group.<sup>27</sup>

A reversible, temperature-dependent behavior of the  $^1\text{H}$  and  $^{31}\text{P}$  NMR resonance patterns was observed (Figure 1). In the slow exchange limit (below  $-70$  °C), a complicated  $^{31}\text{P}$  NMR spectrum was obtained. Interestingly, a two-dimensional  $^{31}\text{P}$ – $^{31}\text{P}$  COSY NMR spectrum at  $-70$  °C has shown the presence of cross-peaks between all multiplets, indicating they are related to only *one* compound and not to a mixture of two or more different complexes.

Integration and simulation of the one-dimensional  $^{31}\text{P}$  NMR spectrum observed at  $-70$  °C strongly suggested

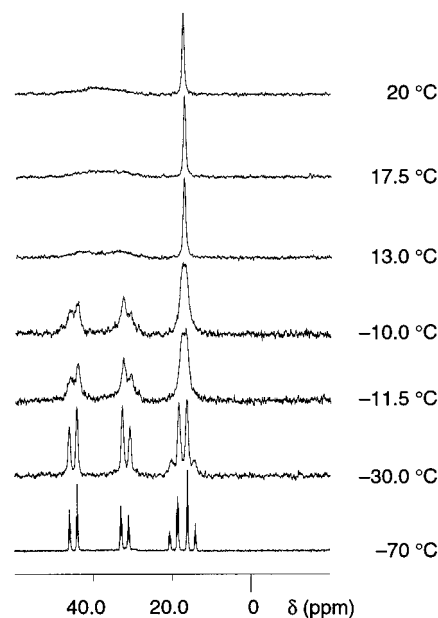


**Figure 1.**  $^{31}\text{P}\{^1\text{H}\}$  NMR spectra of  $[\text{Ru}(\text{PCP})(\text{PCHP})][\text{OTf}]$  (**8**) in  $\text{CD}_2\text{Cl}_2$  at several temperatures.

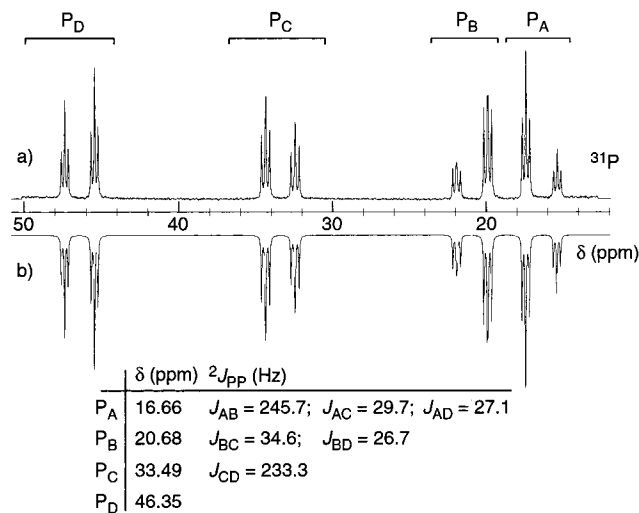


**Figure 2.** (a)  $^{31}\text{P}$  NMR spectrum in  $\text{CD}_2\text{Cl}_2$  of  $[\text{Ru}(\text{PCP})(\text{PCHP})][\text{OTf}]$  (**8**) at  $-70$  °C. (b) Simulated spectrum assuming an ABMN spin system.<sup>30</sup>

the presence of four magnetically and chemically non-equivalent phosphorus atoms (arbitrarily labeled  $P_A$ ,  $P_B$ ,  $P_C$ , and  $P_D$ ), whose spectral distribution, chemical shift, and coupling constants are shown in Figure 2. Comparison of the calculated coupling constants reveals that  $P_A$  is *trans* to  $P_B$ , while  $P_C$  is *trans* to  $P_D$ . This conclusion, in combination with the fact that PCP type ligands are able to adopt a *trans*-spanning  $P,P'$ -coordination mode around a metal center, led to the proposal that a complex containing one *trans*- $P,P'$ -chelated bisphosphinoarene and one cyclometalated bisphosphinoaryl ligand (see **8** in Scheme 2) was formed. Strong supporting evidence for this proposal came from a single-crystal X-ray structure determination of **8**, which was published in a preliminary communication.<sup>28</sup>

Single crystals of  $[\text{Ru}(\text{C}_6\text{H}_3\{\text{CH}_2\text{PPh}_2\}_{2-2,6})(\text{C}_6\text{H}_4\{\text{CH}_2\text{-PPh}_2\}_{2-1,3})][\text{OTf}]$ , **8**, were obtained from a solution in

(27) van Stein, G. C.; van Koten, G.; Vrieze, K.; Brevard, C.; Spek, A. L. *J. Am. Chem. Soc.* **1984**, *106*, 4486–4492.

(28) Dani, P.; Karlen, T.; Gossage, R. A.; Smeets, W. J. J.; Spek, A. L.; van Koten, G. *J. Am. Chem. Soc.* **1997**, *119*, 11317–11318.

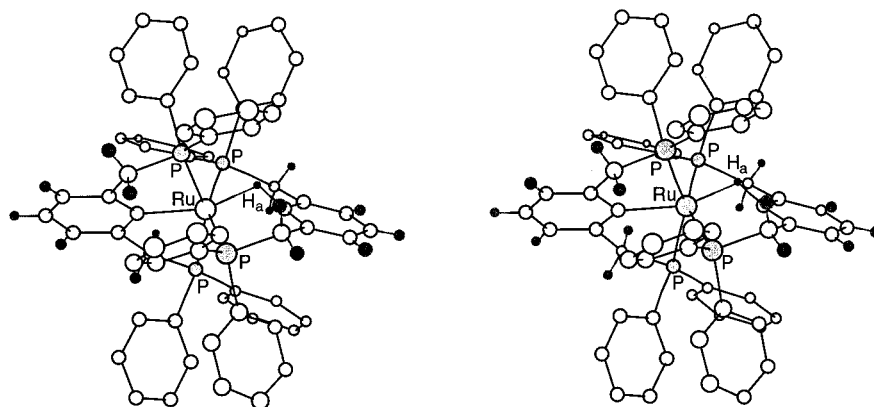


**Figure 3.** Stereoview of the crystal structure of the [Ru(PCP)(PCHP)] cation of **8**. Hydrogen atoms from phenyl groups were omitted for clarity.

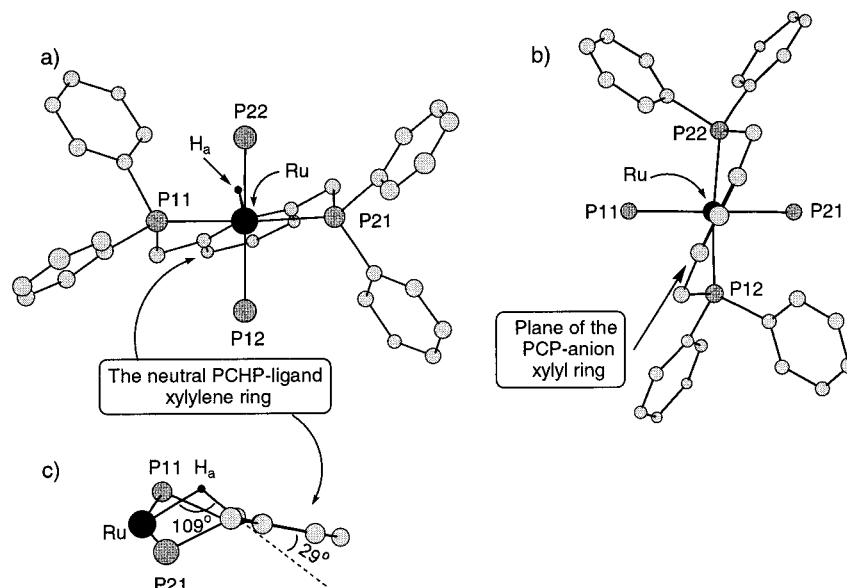


**Figure 4.** Positioning of the aromatic groups in the [Ru(PCP)(PCHP)] cation of **8**. In views a and b the orientation of the various phosphorus atoms are retained. Protons (except  $H_a$ ) were omitted for clarity. (a) View of the neutral PCHP ligand. (b) View of the cyclometalated PCP ligand. (c) Positioning of  $H_a$  of PCHP in relation to the ruthenium center and to the PCP xylylene ring.

dichloromethane layered with a toluene/ether mixture. The molecular structure consists of a bis-*ortho*-phosphinoaryl and a *meta*-bisphosphinoarene ligand bound to one ruthenium atom (Figure 3), as suggested by the solution NMR data. The bisphosphinoaryl ligand is  $\eta^3$ -*P,C,P*-tridentate-bonded to the Ru-center, while the *meta*-bisphosphinoarene ligand is *P,P*-bidentate coordinated. The local symmetry around the ruthenium center is best described as a highly distorted octahedral environment, lacking any kind of symmetry element (hence,  $C_1$  point group symmetry). The location of the hydrogen on C11 ( $H_a$ ) of the *trans*- $\eta^2$ -*P,P*-bonded bisphosphinoarene ligand was clearly refined on the final difference map. The C11– $H_a$  distance is 1.15 Å, which is significantly longer than a normal C–H (aromatic) bond distance. Moreover, the calculated Ru···H distance is 1.76 Å, which is close to the Ru–H bond distance in a classical ruthenium hydride,<sup>29</sup> suggesting a strong Ru– $H_a$  interaction in **8**. Atom  $H_a$  is ca. 30° out of the plane of the PCHP xylylene group, while the C11– $H_a$  bond makes an angle of ca. 109° with the ruthenium center (Figure 4c). The carbon atoms of the neutral

PCHP–xylylene ring are coplanar (see Figure 4a), indicating no loss of aromaticity, as would be expected in the case of a C11  $sp^2 \rightarrow sp^3$  rehybridization resulting from Ru–C11  $\sigma$ -bonding. As can be seen in Figure 4a,b, the *meta*-xylylene rings are not orthogonal to each other. In the neutral PCHP ligand, this part of the molecule is bent toward P12 (Figure 4a). The Ru–P bonds are slightly longer than those in the ruthenium–PCP complex **3**,<sup>21</sup> especially the Ru–P21 bond (2.4432 Å) of the neutral bisphosphinoarene ligand (see Figure 6 for selected bond distances and angles).

It is interesting to note that an alternative way to **8** involves the reaction of **1** with **7** in benzene- $d_6$ . This reaction resulted in complete replacement of all coordinated ligands in **7** by the bisphosphinoarene ligand; that is, the cyclometalated NCN ligand becomes protonated, an  $\eta^3$ -*P,C,P*-bonded bisphosphinoaryl ligand results, and the metal-bound triflate becomes merely a counterion (see Scheme 2). This was confirmed by

(29) Guggenberger, L. J. *Inorg. Chem.* **1973**, *12*, 1317–1322, and references therein.



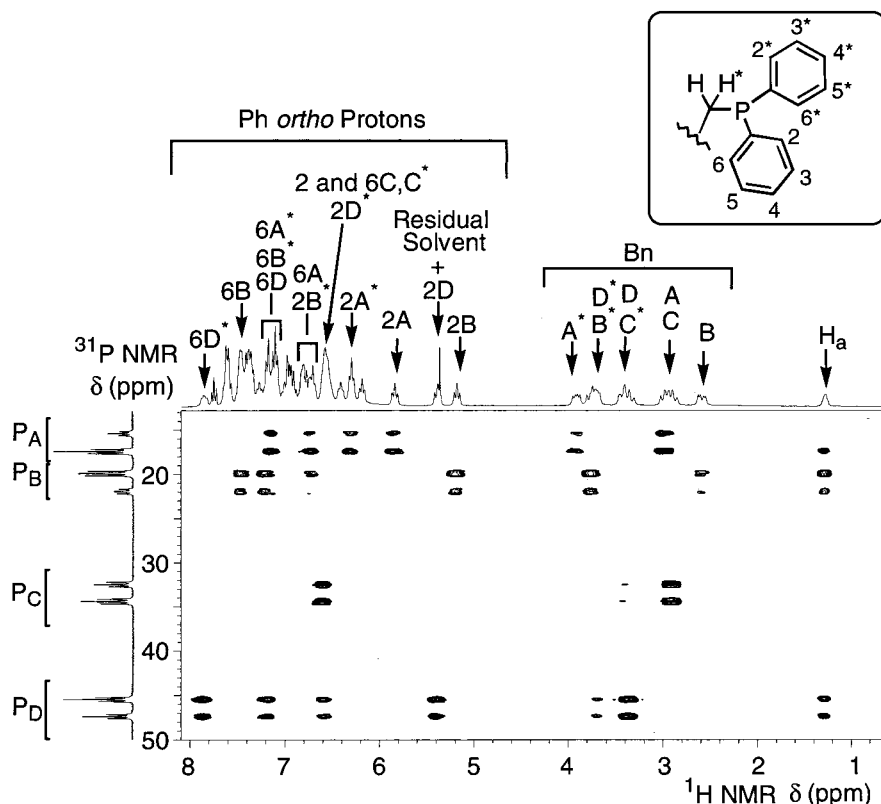


**Figure 5.**  $^{31}\text{P}$ – $^1\text{H}$  COSY NMR spectrum of  $[\text{Ru}(\text{PCP})(\text{PCHP})][\text{OTf}]$  (**8**) in  $\text{CD}_2\text{Cl}_2$  at  $-70\text{ }^\circ\text{C}$ .

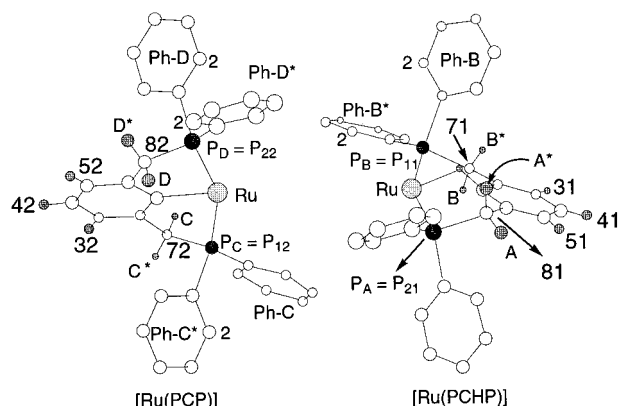


**Figure 6.** Assignments based on the various NMR data realized for  $[\text{Ru}(\text{PCP})(\text{PCHP})][\text{OTf}]$  (**8**). For clarity, the  $[\text{Ru}(\text{PCP})]$  and  $[\text{Ru}(\text{PCHP})]$  fragments are plotted separately (phenyl protons omitted). The *ortho*-position number 2 of the assigned phenyl groups is indicated. Bond distances (Å) and angles (deg.): Ru–P11 2.3732(9), Ru–P21 2.4432(9), Ru–P12 2.3716(9), Ru–P22 2.3575(9), Ru–C12 2.115(3), Ru–H 1.76(4), Ru–C11 2.395(4), C11–H 1.15(4), P11–Ru–P21 152.74(3), P12–Ru–P22 153.64(3), P11–Ru–P12 91.62(3), P11–Ru–P22 95.89(3), C11–Ru–C12 171.47(11), Ru–H–C11 109(3).

comparison of the  $^1\text{H}$  and  $^{31}\text{P}$  NMR spectra of the isolated solid with an authentic sample of **8**. Moreover, in the  $^{31}\text{P}$  NMR spectrum, free  $\text{PPh}_3$  was present, while in the  $^1\text{H}$  NMR spectrum of the reaction mixture, free NCHN was likewise detected. In conclusion, complex **7** is involved in a highly selective exchange reaction<sup>31,32</sup>

(vide infra) and thus can act as a reactive source of ruthenium(II).

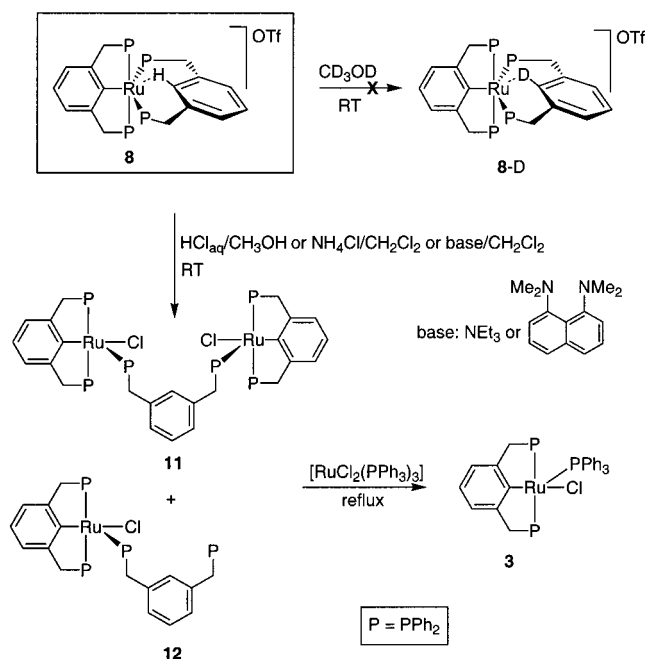
**Reactivity of **8** with Bases and with Chloride Sources.** Attempts to promote abstraction of  $\text{H}_a$  in **8** by reaction with either bases<sup>33</sup> or an acid<sup>20</sup> ( $\text{HCl}$ ), to force the formation of a second C–Ru bond, were not successful (see Scheme 3). This is already evident from the reaction depicted in Scheme 2, in which starting from the Ru–NCN complex **7**, **8** is formed at the expense of the displacement of the bisaminoarene ligand **10**, i.e., of an organic base. Moreover,  $\text{CD}_2\text{Cl}_2$  solutions of **8** in sealed NMR tubes containing stronger amine bases, e.g., triethylamine and “proton sponge”, did not result in any reaction even after two months when kept at temperatures around  $-20\text{ }^\circ\text{C}$ . However, after 4 days at room temperature, the  $^{31}\text{P}$  NMR spectrum (RT) of these samples revealed the disappearance of the broad signals related to the starting material and the presence of a new set of resonances. These new patterns strongly suggested the formation of the already known complexes **11** (d/t at 41.48/83.74 ppm) and **12** (d/t 42.06/83.74 ppm) and a singlet at  $-10.25$  ppm, the latter due to the free diphenylphosphino group; see Scheme 3).<sup>22</sup> A broad singlet at 29.76 was also detected in the same spectrum. The material responsible for this singlet was isolated as a brown solid insoluble in benzene. Most likely, the nature of this material is identical with the paramagnetic impurity observed during the synthesis of **4** with  $\text{AgOTf}$  (see above). Likewise, the  $^1\text{H}$  and  $^{31}\text{P}$  NMR spectra were temperature independent and contained only broad resonances.

(30) Simulation performed using gNMR 3.6, Cherwell Scientific Publishing Limited: Oxford, 1995.

(31) Dani, P.; Albrecht, M.; van Klink, G. P. M.; van Koten, G. *Organometallics* **2000**, *19*, 4468–4476.

(32) Albrecht, M.; Dani, P.; Lutz, M.; Spek, A. L.; van Koten, G. *J. Am. Chem. Soc.*, in press.

(33) Vigalok, A.; Uzan, O.; Shimon, L. J. W.; Ben-David, Y.; Martin, J. M. L.; Milstein, D. *J. Am. Chem. Soc.* **1998**, *120*, 12539–12544.

**Scheme 3. Reactivity of **8** with Bases and with Chloride Sources**

Addition of a solution of HCl in water (ca. 0.2 M) to a solution of **8** in  $\text{CD}_3\text{OD}$  caused immediate precipitation of a green solid. The  $^1\text{H}$  and  $^{31}\text{P}$  NMR spectra of this material in  $\text{C}_6\text{D}_6$  showed that exclusively **11** had been formed (see Scheme 3). A similar result was obtained upon addition of  $\text{NH}_4\text{Cl}$  to a solution of **8** in dichloromethane. In this case, addition of  $[\text{RuCl}_2(\text{PPh}_3)_3]$  and heating the reaction solution overnight yielded the known compound **3** in virtually quantitative yield.

In conclusion, addition of bases or acid to complex **8** did not cause metalation of C11. Instead, phosphine dissociation occurred. The steric demand involved in the formation of four five-membered rings as well as the electronic influence exerted by two *trans* anionic *ipso*-carbons<sup>34,35</sup> may be at the root of the observed behavior. It should be noted that there are examples of ruthenium complexes containing aromatic agostic C–H bonds that do not show any reactivity toward bases or acids.<sup>36</sup>

**Structural Characterization of **8** in Solution by NMR Spectroscopy.** The low molecular symmetry properties found in the solid-state structure of **8** is in good agreement with the observed  $^{31}\text{P}\{^1\text{H}\}$  NMR spectrum recorded in  $\text{CD}_2\text{Cl}_2$  solution (Figure 2). A series of two-dimensional NMR studies were carried out at the slow exchange limit temperatures ( $-70$  to  $-90$  °C) to further our understanding of the nature of the interaction between  $\text{H}_a$  and the ruthenium center. An additional objective was to probe the possible fluxional behavior of **8**. It is important to note that the most informative proton nuclei, i.e., those that provide the most useful structural information, are those that are in close proximity to the ruthenium metal center, i.e.,  $\text{H}_a$ , the phenyl *ortho* and benzylic protons. Therefore,

our first goal was to locate these protons in the  $^1\text{H}$  NMR spectrum of **8**.

Initially, the complexity of the one-dimensional  $^1\text{H}$  NMR spectrum hampered the precise location of the chemical shift of  $\text{H}_a$ . Interestingly,  $\text{H}_a$  is the only hydrogen atom in **8** capable of showing reasonable through-bond coupling with all four phosphorus atoms, for it is only two bonds apart from each of them. A two-dimensional  $^{31}\text{P}-^1\text{H}$  COSY NMR spectrum was recorded at  $-70$  °C (Figure 5). Despite the apparent spectral complexity of the NMR spectrum of **8**, the location of all the important protons (i.e., their chemical shift and information on which type of phosphorus they are related to) can be extracted (Figure 6). The aromatic proton  $\text{H}_a$  is found at 1.23 ppm and shows cross-peaks with the  $\text{P}_A$ ,  $\text{P}_B$ , and  $\text{P}_D$  phosphorus nuclei. Therefore,  $\text{H}_a$  is unambiguously bonded to the Ru center. The reasons for the nonpresence of a cross-peak between  $\text{H}_a$  and  $\text{P}_C$  were not further investigated. To substantiate the agostic C– $\text{H}_a\cdots\text{Ru}$  interaction, complex **8-D** was synthesized by reacting **4** with the deuterated H–PCDP ligand **1-D** (isotopic purity > 99%) in  $\text{CH}_2\text{Cl}_2$  at room temperature (Scheme 2). Indeed, the signal located at 1.23 ppm ( $^1\text{H}$  NMR) was the one affected in the  $^1\text{H}$  NMR spectrum of **8-D**, confirming the findings of the  $^{31}\text{P}-^1\text{H}$  COSY NMR spectrum. However, it was observed that a small proton resonance was still visible at 1.23 ppm, indicating that the partial replacement of the deuterium by hydrogen had occurred (less than 10% is estimated). The  $^2\text{H}\{^1\text{H}\}$  NMR spectrum (RT) showed a broad signal centered at 1.23 ppm and a small one at 7.35 ppm. Due to the broadness of the  $^2\text{H}$  NMR spectrum, it is difficult to assign the latter proton with certainty. However, the deuterium scrambling occurred in a very selective manner and is probably caused by an intramolecular process.

Figure 5 also reveals that each of the diastereotopic benzylic protons appears at distinct chemical shift values. They were arbitrarily labeled after the name of the respective phosphorus nuclei (Bn-A, -A\*; Bn-B, -B\*; Bn-C, -C\*; Bn-D, -D\*). The symbol \* was used to denote benzylic (and phenyl) protons related to the same phosphorus atom having a diastereotopic relationship (see inset of Figure 5).

The cross-peaks related to the aromatic region (5–8 ppm) of the  $^1\text{H}$  NMR spectrum (Figure 5) are all due to couplings with phenyl *ortho* protons. Different chemical shifts are expected for *ortho* protons situated at different phenyl groups, even if the phenyl groups are bonded to the same phosphorus atom, because, as is the case of the benzylic protons, the phenyl groups can be divided into diastereotopic pairs (see Figure 4a,b). However, as can be seen in Figure 5,  $\text{P}_A$ ,  $\text{P}_B$ , and  $\text{P}_D$  have four cross-peaks in the aromatic region of the  $^1\text{H}$  NMR spectrum, indicating nonequivalence between *ortho* protons related to the same phenyl ring. In the case of  $\text{P}_C$ , where there is only one cross-peak, most likely the situation is the same as with  $\text{P}_A$ ,  $\text{P}_B$ , and  $\text{P}_D$ , and coincidence is causing the chemical shift equivalence among all *ortho* protons.

$^1\text{H}-^1\text{H}$  COSY and  $^1\text{H}-^1\text{H}$  TOCSY NMR spectra confirmed the assignments related to the benzylic protons of **8**. Furthermore, these spectra made clear which *ortho* protons pertained to a specific phenyl ring

(34) Steffey, B. D.; Miedaner, A.; Maciejewski-Farmer, M. L.; Bernatis, P. R.; Herring, A. M.; Allured, V. S.; Carperos, V.; DuBois, D. L. *Organometallics* **1994**, *13*, 4844–4855.

(35) Pape, A.; Lutz, M.; Müller, G. *Angew. Chem., Int. Ed. Engl.* **1994**, *33*, 2281–2284.

(36) Perera, S. D.; Shaw, B. L. *J. Chem. Soc., Dalton Trans.* **1995**, 3861–3866.

**Table 1.**  $^1\text{H}$  NMR Chemical Shift and Assignments of  $[\text{Ru}(\text{PCP})(\text{PCHP})][\text{OTf}]$  (**8**)<sup>a</sup>

	phenyl protons					benzylic proton
	<i>o</i> -H	<i>o</i> *-H	<i>m</i> -H	<i>m</i> *-H	<i>p</i> -H	
A	5.78	6.68	6.35	6.68	6.78	2.95
A*	6.24	7.08	7.03	7.36–7.46	<i>b</i>	3.86
B	5.15	7.39	6.13	7.05	6.85	2.52
B*	6.65	7.13	7.33	<i>a</i> )	<i>b</i>	3.71
C	6.53	6.53	<i>a</i> )	<i>a</i> )	<i>b</i>	2.84
C*						3.35
D	5.34	7.10	6.24	6.88–7.10	6.88	3.31
D*	6.50	7.79	6.50	7.57	7.20	3.67
			H-3n	H-4n	H-5n	H <sub>a</sub>
PCHP ( <i>n</i> = 1)			7.33	7.75	7.33	1.22
PCP ( <i>n</i> = 2)			6.92	<i>b</i>	7.12	

<sup>a</sup> For the labeling scheme; see Figure 6. <sup>b</sup> It was not possible to locate this proton with certainty in the  $^1\text{H}$  NMR spectrum with the available data.

and the chemical shift of the protons H-31, H-41, and H-51 (for the numbering, see Scheme 2). Interestingly, H-31 and H-51 showed cross-peaks with benzylic protons A, B, and B\*. Consequently, P<sub>A</sub> and P<sub>B</sub> (and the associated benzylic and phenyl *ortho* protons) are related to the *P,P'* (chelate)-bonded PCHP ligand, while P<sub>C</sub> and P<sub>D</sub> belong to the cyclometalated PCP-anionic fragment. These findings are summarized in the  $^1\text{H}$  NMR spectrum of Figure 5 and in Table 1.

The nature of the C11–H<sub>a</sub> interaction followed from the results of a  $^{13}\text{C}$ – $^1\text{H}$  COSY NMR spectrum of **8** at –70 °C. This experiment revealed a cross-peak involving H<sub>a</sub> and C11 ( $\delta_{\text{C}}$  = 118 ppm). The C11 chemical shift is about 12 ppm to higher field in comparison with this resonance in the parent PCHP ligand. In conclusion,  $^{31}\text{P}$ – $^1\text{H}$  and  $^{13}\text{C}$ – $^1\text{H}$  COSY established that H<sub>a</sub> interacts with both Ru and C11. These characteristics are typical for agostic systems and explain the reduced magnitude of the C–H coupling constant. Gated decoupling experiments<sup>37</sup> revealed that the actual value is 112 Hz, which is 46 Hz smaller than this coupling constant in free PCHP. The observed  $\Delta J$  is in the normal range for complexes containing agostic contacts.<sup>20</sup>

The data gathered so far suggest that the structure of **8** in solution and in the solid state are both very similar. To substantiate this conclusion further, several  $^1\text{H}$  NOESY and ROESY and  $^{31}\text{P}$  NOESY (EXSY) NMR spectra of **8** were recorded at two different temperatures (–70 and –90 °C). The experiments employed different mixing times in an attempt to address the dynamic behavior of **8** in solution. We were particularly interested in determining whether H<sub>a</sub> could be exchanged between C11 and C12 (the C<sub>ipso</sub>). If this happens on the NMR time scale of the applied techniques, one would expect exchange cross-peaks between A,B, and C,D type protons in an EXSY spectrum.

Interestingly, all the  $^1\text{H}$  NOESY spectra contained strong cross-peaks having phase equal to the spectral diagonal. Unfortunately, this situation makes it impossible to differentiate between NOE and chemical exchange cross-peaks. This problem could be solved by using ROESY NMR spectroscopy, in which cross-peaks due to chemical exchange appear with an inverted phase in relation with cross-peaks arising from NOE effects.<sup>38</sup>

These measurements showed that H<sub>a</sub> lacks any chemical exchange cross-peak at temperatures lower than –70 °C, while this proton does show NOE cross-peaks with A, A\*, B, and B\* benzylic protons. This latter observation is in concert with the  $^1\text{H}$ – $^1\text{H}$  COSY and TOCSY analysis, which indicated that A and B type protons are related to the *P,P'*-coordinated PCHP ligand. Except for the benzylic proton A\*, all other cross-peaks between H<sub>a</sub> and benzylic protons were relatively weak. This parallels the observation that in the crystal structure of **8** all distances between H<sub>a</sub> and the respective benzylic protons of the PCHP ligand fall in a narrow range (3.46–3.53 Å) except for the much shorter distance (2.64 Å) of the proton connected to benzylic carbon C81. Consequently, this proton was assigned as A\*. Following similar procedures, the identity of most of the aromatic ring carbons and protons could be established (Figure 6).

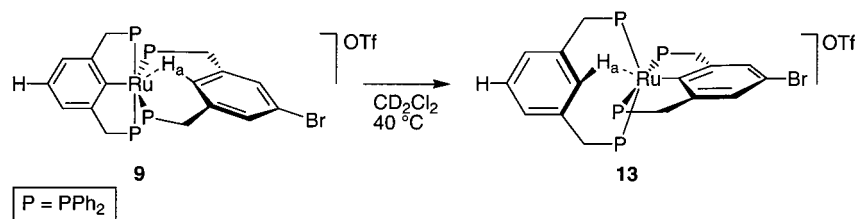
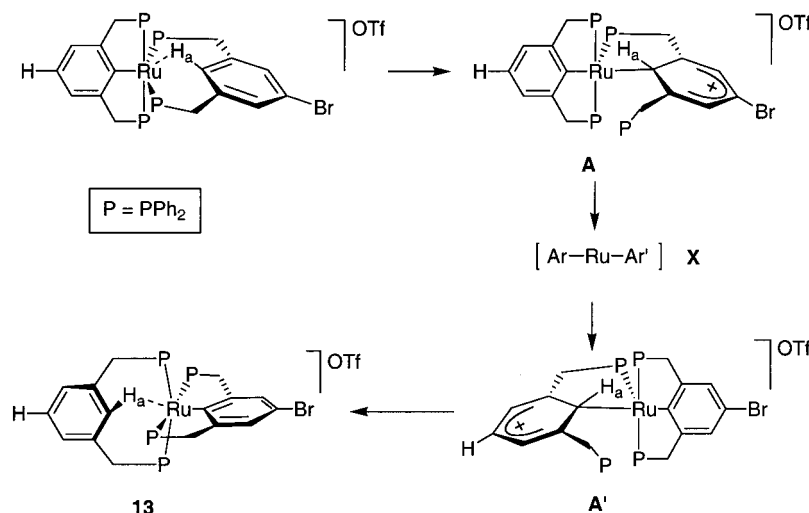
Whereas the  $^1\text{H}$  ROESY spectrum between –70 and –90 °C showed no evidence for chemical exchange involving H<sub>a</sub>, it does show exchange cross-peaks within benzylic and within aromatic A $\leftrightarrow$ A\*, B $\leftrightarrow$ B\*, C $\leftrightarrow$ C\*, D $\leftrightarrow$ D\*, A(\*) $\leftrightarrow$ B(\*), and C(\*) $\leftrightarrow$ D(\*) type protons. However, exchange between the two groups (i.e., A,B $\leftrightarrow$ C,D) was not observed. This was confirmed by  $^{31}\text{P}$  NOESY (EXSY) spectroscopy, in which the exchange P<sub>A</sub> $\leftrightarrow$ P<sub>B</sub> and P<sub>C</sub> $\leftrightarrow$ P<sub>D</sub> is clearly evident but not P<sub>A,B</sub> $\leftrightarrow$ P<sub>C,D</sub>. These results indicate that on the time scale of the applied NMR techniques the dynamic behavior in **8** is mainly caused by the movement of the *trans-P,P'*-bidentate-bonded PCHP ligand. This is not surprising if one considers that the bidentate chelate is likely much more flexible with respect to the tridentate  $\eta^3$ -*P,C,P'*-coordinated (formally monoanionic) PCP ligand. However, it was not possible to establish whether the dynamic behavior was caused by one single or several simultaneous mechanisms. Finally, it should be noted that exchange of H<sub>a</sub> between C11 and C12, which would represent a degenerative process from the point of view of **8**, either does not occur or it does with a rate too small to be detected by the techniques used. To verify whether such exchange could be triggered at room temperature (or above) and on a laboratory time frame, some chemical experiments were performed involving complexes analogous to **8**.

**Chemical Experiments Involving Exchange Reactions between  $\eta^3$ -*P,C,P'*-Coordinated PCP and *P,P'*-Coordinated PCHP Ligands.** To study whether displacement of H<sub>a</sub> from C11 to C12 could be a feasible process, a different chelate-bonded *meta*-bisphosphinoarene ligand with a *para* substituent R  $\neq$  H was used. In this case, migration of H<sub>a</sub> between C11 and C12 would cause the formation of distinct compounds,  $[\text{Ru}(\text{PCP})(\text{R}-\text{PCHP})][\text{OTf}]$  and  $[\text{Ru}(\text{R}-\text{PCP})(\text{PCHP})][\text{OTf}]$ , which each would have unique spectroscopic features. Therefore, complex **9** was synthesized in a reaction at room temperature (in  $\text{CH}_2\text{Cl}_2$ ) between  $[\text{Ru}(\text{OTf})(\text{PCP})(\text{PPh}_3)]$  (**4**) and the *para*-bromo-substituted ligand **2** (Scheme 2). Like the analogous complex **8**, **9** is a yellow solid with very similar spectroscopic features and is highly fluxional in solution. In the  $^{31}\text{P}$  NMR spectrum

(37) Friebolin, H. *Basic One- and Two-Dimensional NMR Spectroscopy*, 2nd ed.; VCH: Weinheim, Germany, 1993; p 127.

(38) (a) Braun, S.; Kalinowski, H.-O.; Berger, S. *100 and More Basic NMR Experiments. A Practical Course*; VCH: Weinheim, Germany, 1996; p 330. (b) Freeman, R. *Spin Choreography: Basic Steps in High-Resolution NMR*; Spektrum, Oxford, England, 1997; p 295.



**Scheme 4. Isomerization Reaction Observed with Complex 9****Scheme 5. Mechanistic Proposal for the Isomerization Reaction Observed with 9**

at  $-70\text{ }^{\circ}\text{C}$ , a set of four multiplets of an ABMN spin system is observed, and in the  $^1\text{H}$  NMR spectrum at the same temperature a broad singlet is present at 1.08 ppm. The same NMR analyses performed with **8** were used to characterize **9**. In this way, the signal at 1.08 ppm in the  $^1\text{H}$  NMR spectrum was clearly established as the resonance frequency of proton  $\text{H}_a$  in complex **9**. In a sealed NMR tube, a solution of **9** in  $\text{CD}_2\text{Cl}_2$  was kept at  $40\text{ }^{\circ}\text{C}$  for 40 min. After this period, a  $^1\text{H}$  NMR spectrum at  $-70\text{ }^{\circ}\text{C}$  showed the presence of a second broad singlet at 1.23 ppm, the same chemical shift in which  $\text{H}_a$  of **8** is observed. In the  $^{31}\text{P}$  NMR spectrum, also at  $-70\text{ }^{\circ}\text{C}$ , two ABMN spin systems were present. Their independence was confirmed by a  $^{31}\text{P}$ – $^{31}\text{P}$  COSY NMR spectrum. The logical explanation for these observations is that **9** is being isomerized into complex **13** (Scheme 4). No isomerization reaction was observed at temperatures below  $25\text{ }^{\circ}\text{C}$ . Complete conversion of **9** into **13** could not be achieved due to decomposition of these complexes in dichloromethane solution in a way similar to that observed for pure **8**.

The reaction depicted in Scheme 4 shows that the conversion of the metalated site into the nonmetalated one is possible in the case of complex **9**. The fact that the process was only effective at temperatures above  $25\text{ }^{\circ}\text{C}$  indicates that the energy barrier for the interconversion is relatively high. The greater thermodynamic stability of **13** over **9** is likely to be the result of electronic differences caused by the nature of the *para*-substituent R (H or Br). In terms of electrophilic aromatic substitution, halogens are considered *ortho/para* directors and electron-withdrawing substituents. However, there are two pieces of evidence that suggest that the C– $\text{H}_a$  carbon atom in **9** can have an electron density greater than the same carbon in **8**. The first one

comes from the chemical shift of this particular carbon in the  $^{13}\text{C}$  NMR spectrum of the *free* ligands **1** ( $\delta = 130.46\text{ ppm}$ )<sup>31</sup> and **2** ( $\delta = 129.38\text{ ppm}$ ).<sup>22</sup> Therefore, there is an upfield shift ( $\Delta\delta = \delta_1 - \delta_2$ ) 1.08 ppm for the carbon of ligand **2**, suggesting an increase of the electron density over this carbon. Similar analysis has already been employed for other compounds containing NCN<sup>39</sup> and PCP<sup>40</sup> “pincer” ligands.

The second piece of evidence is related to the observed difference in chemical shift of  $\text{H}_a$  in complexes **8** or **13** ( $\delta\text{H}_a = 1.23\text{ ppm}$ ) and **9** ( $\delta\text{H}_a = 1.08\text{ ppm}$ ) in the  $^1\text{H}$  NMR spectrum. It is reasonable to assume that these complexes have similar structures, and therefore, the origin for such chemical shift difference should be electronic in nature. Hence, the shielding effect observed in the chemical shift of  $\text{H}_a$  in **9** also suggests that the C– $\text{H}_a$  bond in this complex has a higher electron density than the same bond in **8** or **13**. Taking into account these two factors, the isomerization shown in Scheme 4 is likely to happen via an electrophilic aromatic substitution mechanism involving arenium-type intermediates, like **A** and **A'**, and a transition state (or very reactive intermediate) containing two *trans* C12–Ru–C11 bonds (**X**, Scheme 5). The participation of arenium species in the formation of metal–carbon bonds has been the subject of a number of studies involving late transition metal complexes of “pincer” ligands.<sup>41,42</sup> Furthermore, the transfer of an aromatic proton of a PCHP ligand to an  $\eta^3\text{-}N,C,N'$  metal bonded NCN ligand has been observed and identified by us as transcyclo-

(39) van de Kuil, L. A.; Luitjes, H. Grove, D. M.; Zwikker, J. W.; van der Linden, J. G. M.; Roelofsen, A. M.; Jenneskens, L. W.; Drenth, W.; van Koten, G. *Organometallics* **1994**, *13*, 468–477.

(40) Weisman, A.; Gozin, M.; Kraatz, H.-B.; Milstein, D. *Inorg. Chem.* **1996**, *35*, 1792–1797.



metalation (TCM) reactions.<sup>31</sup> These TCM reactions have been applied as a tool for the synthesis of Ru–PCP<sup>31</sup> and Pt–PCP<sup>32</sup> complexes as well as for the alternative synthesis of **8** from the reaction of [RuOTf(NCN)(PPh<sub>3</sub>)], **7**, with PCHP (**1**) presented here; see Scheme 2. In these cases, there are strong indications that the proton transfer from the PCHP to the NCN ligands occurs via an intramolecular mechanism assisted by the amino groups of the NCN ligand. Whether the same mechanism can be operative here for the case of **9**, in which only phosphorus ligands are present, is still a matter of further studies. However, it should be noted that exchange of H<sub>a</sub> in **8** by deuterium via simple solubilization of this complex in CD<sub>3</sub>OD was not observed.

It is very likely that the same isomerization observed with **9** is also happening with **8**. In fact, an equilibrium should be present between the two possible (degenerate) isomers. At low temperatures (around –70 °C), the rate constant for this process should be quite small since one does not observe any characteristic cross-peaks in the <sup>1</sup>H and <sup>31</sup>P NOESY analysis involving exchange of the type A,B↔C,D. Indeed, the need for heating **9**, which leads to **13**, is a reflection of this aspect.

## Conclusions

We have detailed the synthesis, characterization, and reactivity of ruthenium complexes containing bisphosphinoaryl and biphosphinoarene ligands in which one is  $\eta^3$ -P,C,P' bonded to the metal and the other is  $\eta^2$ -P,P' bonded via the phosphorus groups only. The aromatic C–H<sub>a</sub> bond (see Figure 3) of the bidentate meta-bisphosphinoarene ligand has an agostic interaction with the ruthenium center. <sup>31</sup>P–<sup>1</sup>H COSY NMR spectroscopy was successfully used in order to precisely locate the resonance of this proton in the <sup>1</sup>H NMR spectrum. Compounds containing agostic contacts are frequently indicated as possible intermediates in metal–carbon bond formation. In the work reported herein, it was possible to observe the actual formation of a new Ru–C bond at the expense of another Ru–C bond, probably via an electrophilic aromatic pathway. Finally, complex **7** (containing a cyclometalated terdentate bisaminoaryl ligand) was introduced as a new ruthenium starting material capable of the delivery of a Ru<sup>II</sup> nucleus to form new cyclometalated species.

## Experimental Section

**General Comments.** All experiments were conducted under dry nitrogen atmosphere using standard Schlenk techniques. Solvents were dried over appropriate materials and distilled prior to use. [RuCl<sub>2</sub>(PPh<sub>3</sub>)<sub>3</sub>],<sup>43</sup> **1**,<sup>4</sup> **5**,<sup>44</sup> and **8**<sup>28</sup> were

synthesized as described in the literature. Me<sub>3</sub>SiOTf and *n*BuLi were purchased commercially. <sup>1</sup>H, <sup>13</sup>C, and <sup>31</sup>P NMR spectra were recorded on a Varian Unity Inova 300 MHz spectrometer using standard pulse sequences. Chemical shifts are reported in ppm from (CH<sub>3</sub>)<sub>4</sub>Si or from the solvent peak (<sup>1</sup>H and <sup>13</sup>C NMR spectra) and from a capillary containing 85% H<sub>3</sub>PO<sub>4</sub> (<sup>31</sup>P NMR spectra). All deuterated solvents were degassed prior to use (4 times) using the freeze–pump–thaw methodology and stored under nitrogen over 4 Å molecular sieves. The NMR experiments with complexes such as **8** were typically performed by transferring ca. 30 mg of the complex dissolved in 0.7 cm<sup>3</sup> of CD<sub>2</sub>Cl<sub>2</sub> to a 5 mm NMR tube containing a glass stopper. Except for the NOESY, TOCSY, and ROESY experiments, all other two-dimensional experiments were performed in a non-phase-sensitive mode. The second pulse in the <sup>1</sup>H–<sup>1</sup>H COSY experiment was set to 45°. Normal-range <sup>13</sup>C–<sup>1</sup>H COSY spectra were recorded considering <sup>1</sup>J<sub>HC</sub> = 140 Hz. T<sub>1</sub> times for protons of complexes such as **8** fall in the range 0.4–1.5 s. <sup>1</sup>H NOESY experiments were recorded with mixing times 0.2, 0.5, 0.8, 1.0, and 1.5 s and <sup>1</sup>H ROESY with mixing times of 0.1 and 0.5 s. <sup>31</sup>P EXSY spectra were recorded with mixing times of 0.5 and 1.0 s.

**Synthesis of C<sub>6</sub>H<sub>3</sub>(CH<sub>2</sub>PPh<sub>2</sub>)<sub>2</sub>-1,3-D-2 (**1-D**).** To a solution of C<sub>6</sub>H<sub>3</sub>(CH<sub>2</sub>Br)<sub>2</sub>-1,3-D-2 in xylene was added 2 equiv of EtOPPh<sub>2</sub>. After 2 h of heating to reflux temperature, the volatiles were removed and the remaining residue was extracted with hexane. This resulted in the formation of the corresponding phosphine oxide as a white solid. The reduction was performed by adding an excess of HSiCl<sub>3</sub> dropwise to a hot solution of the phosphine oxide in benzene. The volatiles were removed in vacuo, and the oily residue was treated with hexane to induce crystallization. The formed white waxlike precipitate was filtered off and dried under vacuum. Yield: 70% (based on C<sub>6</sub>H<sub>3</sub>(CH<sub>2</sub>Br)<sub>2</sub>-1,3-D-2). <sup>1</sup>H NMR (300 MHz, CDCl<sub>3</sub>): δ 3.41 (s, 4H, CH<sub>2</sub>), 6.89 (m, 2H, CH-4,6), 7.06 (t, 1H, CH-5, <sup>3</sup>J<sub>HH</sub> = 8 Hz), 7.38 (m, meta-H of PPh<sub>2</sub>), 7.44 (m, para-H of PPh<sub>2</sub>), 7.48 (m, ortho-H of PPh<sub>2</sub>). <sup>13</sup>C{<sup>1</sup>H} NMR (75 MHz, CDCl<sub>3</sub>): δ 35.89 (d, CH<sub>2</sub>, <sup>1</sup>J<sub>CP</sub> = 16 Hz), 126.99 (m, CH-4,6), 128.12 (s, CH-5), 128.34 (d, meta-H of PPh<sub>2</sub>, <sup>3</sup>J<sub>CP</sub> = 7 Hz), 128.65 (s, para-H of PPh<sub>2</sub>), 132.90 (d, ortho-H of PPh<sub>2</sub>, <sup>2</sup>J<sub>CP</sub> = 18 Hz), 137.33 (dd, C-1,3, <sup>2</sup>J<sub>CP</sub> = 8 Hz, <sup>4</sup>J<sub>CP</sub> = 2 Hz), 138.33 (d, C–P, <sup>1</sup>J<sub>CP</sub> = 15 Hz). <sup>31</sup>P{<sup>1</sup>H} NMR (121 MHz, CDCl<sub>3</sub>): δ –9.52 (s).

**Synthesis of C<sub>6</sub>H<sub>3</sub>(CH<sub>2</sub>PPh<sub>2</sub>)<sub>2</sub>-3,5-Br-1 (**2**).** A three-neck 500 cm<sup>3</sup> round-bottom flask containing an ammonia condenser and a magnetic stirring bar was connected to a nitrogen line and then immersed in an acetone–dry ice bath. Condensing of ammonia (about 250 cm<sup>3</sup>) was followed by addition of small sodium cuts (1.38 g, 60 mmol). After 30 min, solid PPh<sub>3</sub> (7.87 g, 30 mmol) was added to the intense blue-colored solution. The color of the mixture almost immediately changed to pale yellow. After 40 min, dry ammonium bromide (2.94 g, 30 mmol) was slowly added followed after 15 min by solid C<sub>6</sub>H<sub>3</sub>(CH<sub>2</sub>Br)<sub>2</sub>-3,5-Br-1 (5.14 g, 15 mmol), which was added in a single portion. The acetone–dry ice bath was then removed. After evaporation of the ammonia (4 h), degassed water (200 cm<sup>3</sup>) and diethyl ether (200 cm<sup>3</sup>) were added. The organic layer was transferred to another round-bottom flask using a cannula. The water layer was extracted with diethyl ether (2 × 100 cm<sup>3</sup>). The combined organic fractions were dried over magnesium sulfate. The magnesium sulfate was filtered off, and the volatiles were removed in vacuo, resulting in the formation of a white solid. Sometimes, crystallization from MeOH is necessary. Yield: 60–70%. Anal. Calcd (Found) for C 69.45 (69.41), H 4.92 (4.88). Mp: 95–97 °C. <sup>1</sup>H NMR (200 MHz, CDCl<sub>3</sub>): δ 3.26 (s, 4H, CH<sub>2</sub>), 6.75 (s, 1H, CH ortho to both CH<sub>2</sub>PPh<sub>2</sub> groups), 6.91 (s, 2H, BrCCH), 7.20–7.45 (m, 20H, aromatic protons). <sup>13</sup>C{<sup>1</sup>H} NMR (CDCl<sub>3</sub>, 75 MHz): δ 35.94 (d, CH<sub>2</sub>, <sup>1</sup>J<sub>CP</sub> = 17 Hz), 122.15 (s, CBr), 128.71 (d, meta-C of PPh<sub>2</sub>, <sup>3</sup>J<sub>CP</sub> = 7 Hz), 129.14 (s, para-C of PPh<sub>2</sub>), 129.38 (t, CH-4, <sup>3</sup>J<sub>CP</sub> = 7 Hz), 130.14 (d, Br–C–CH), 133.14 (d, ortho-C of PPh<sub>2</sub>, <sup>2</sup>J<sub>CP</sub> =

(41) (a) van Koten, G.; Timmer, K.; Noltes, J. G.; Spek, A. L. *J. Chem. Soc., Chem. Commun.* **1978**, 250–252. (b) Grove, D. M.; van Koten, G.; Louwen, J. N.; Noltes, J. G.; Spek, A. L.; Ubbels, H. J. C. *J. Am. Chem. Soc.* **1982**, 104, 6609–6616. (c) Albrecht, M.; Gossage, R. A.; Spek, A. L.; van Koten, G. *J. Am. Chem. Soc.* **1999**, 121, 11898–11899.

(42) (a) van der Boom, M. E.; Ben-David, Y.; Milstein, D. *J. Am. Chem. Soc.* **1999**, 121, 6652–6656. (b) Vigalok, A.; Shimon, L. J. W.; Milstein, D. *J. Am. Chem. Soc.* **1998**, 120, 477–483.

(43) Hallman, P. S.; Stephenson, T. A.; Wilkinson, G. *Inorg. Synth.* **1970**, 12, 237.

(44) Sutter, J.-P.; James, S. L.; Steenwinkel, P.; Grove, D. M.; Veldman, N.; Smeets, W. J. J.; Spek, A. L.; van Koten, G. *Organometallics* **1996**, 15, 941–948.

19 Hz), 138.07 (d,  $C_{\text{quat}}$  of  $\text{PPh}_2$ ,  $^1J_{\text{CP}} = 15$  Hz), 139.77 (d,  $C-\text{CH}_2\text{PPh}_2$ ,  $^2J_{\text{CP}} = 9$  Hz).  $^{31}\text{P}\{^1\text{H}\}$  NMR ( $\text{CDCl}_3$ , 81 MHz):  $\delta$  -9.07 (s).

**Synthesis of  $[\text{Ru}(\text{OTf})(\text{C}_6\text{H}_3\{\text{CH}_2\text{NMe}_2\}_2\text{-2,6})(\text{PPh}_3)]$  (7).** To a Schlenk tube containing **5** (0.1870 g, 0.32 mmol) dissolved in benzene (30  $\text{cm}^3$ ) was added  $\text{Me}_3\text{SiOTf}$  (0.2  $\text{cm}^3$ , 0.96 mmol). After stirring for 22 h at room temperature, the initially blue solution became purple. The volatiles were pumped off, and the solid residue was washed with pentane ( $5 \times 3$   $\text{cm}^3$ ) and dried in a vacuum, yielding a purple solid. Yield: 0.1577 g (70%).  $^1\text{H}$  NMR (200 MHz,  $\text{C}_6\text{D}_6$ ):  $\delta$  1.97 (s, 6H,  $\text{CH}_3$ ), 2.00 (s, 6H,  $\text{CH}_3$ ), 2.35 (s, 4H,  $\text{CH}_2$ ), 6.72 (d, 2H, H-3,5,  $^3J_{\text{HH}} = 7.4$  Hz), 6.85–7.10 (m, 11H, *m,p*-H of  $\text{PPh}_3$  protons and H-4), 7.50–7.62 (m, 6H, *o*-H of  $\text{PPh}_3$  protons).  $^{31}\text{P}\{^1\text{H}\}$  NMR (81 MHz,  $\text{C}_6\text{D}_6$ ):  $\delta$  87.23 (s).

**Synthesis of  $[\text{Ru}(\text{PCP})(\text{PCHP})][\text{OTf}]$  (8) from  $[\text{Ru}(\text{OTf})(\text{NCN})\text{PPh}_3]$  (7).** PCHP (**1**, 1.5 equiv) was added to a solution of **7** in  $\text{C}_6\text{D}_6$  at RT. The resulting solution was kept at 60 °C for 12 h. During this period, the purple solution

became green colored, and gradually yellow crystals of **8** separated out. These crystals were collected and analyzed by  $^1\text{H}$  and  $^{31}\text{P}$  NMR spectroscopy in  $\text{CD}_2\text{Cl}_2$ , which confirmed the exclusive formation of **8**.

**Synthesis of  $[\text{Ru}(\text{PCP})(\text{PCDP})][\text{OTf}]$  (8-D) and  $[\text{Ru}(\text{PCP})(\text{Br-PCHP})][\text{OTf}]$  (9).** Both **8-D** and **9** were synthesized by the reported procedure for **8**<sup>28</sup> using ligands **1-D** (for **8-D**) and 1- $\text{C}_6\text{H}_3(\text{CH}_2\text{PPh}_2)_2\text{-3,5-Br-1}$ , **2** (for **9**). Characterization of **9**:  $^1\text{H}$  NMR (300 MHz,  $\text{CD}_2\text{Cl}_2$ , -70 °C):  $\delta$  1.08 (bs, 1H,  $\text{H}_a$ ), 2.35–4.20 (m, 8H,  $\text{CH}_2$ ), 5.0–8.20 (m, 45H, aromatic protons).  $^{31}\text{P}\{^1\text{H}\}$  NMR (121 MHz,  $\text{CD}_2\text{Cl}_2$ , -70 °C):  $\delta$  16.55 (dt, 1P,  $\text{P}_A$ ,  $^2J_{\text{PP}} = 274$  and 29 Hz), 20.43 (dt, 1P,  $\text{P}_B$ ,  $^2J_{\text{PP}} = 274$  and 30 Hz), 30.89 (dt, 1P,  $\text{P}_C$ ,  $^2J_{\text{PP}} = 230$  and 31 Hz), 45.79 (dt, 1P,  $\text{P}_D$ ,  $^2J_{\text{PP}} = 230$  and 27 Hz). Anal. Calcd (Found) for  $\text{C}_{65}\text{H}_{54}\text{BrF}_3\text{O}_3\text{P}_4\text{RuS} \cdot 1.5\text{CH}_2\text{Cl}_2$ : C 56.87 (56.25), H 4.09 (4.12), Br 5.69 (5.65), P 8.82 (8.72).

OM0005001